

## A simple and accurate model for Love wave based sensors: Dispersion equation and mass sensitivity

Jiansheng Liu

Citation: *AIP Advances* **4**, 077102 (2014); doi: 10.1063/1.4886773

View online: <http://dx.doi.org/10.1063/1.4886773>

View Table of Contents: <http://scitation.aip.org/content/aip/journal/adva/4/7?ver=pdfcov>

Published by the *AIP Publishing*

---

### Articles you may be interested in

[Integrated active mixing and biosensing using low frequency vibrating mixer and Love-wave sensor for real time detection of antibody binding event](#)

*J. Appl. Phys.* **109**, 094701 (2011); 10.1063/1.3576113

[Theoretical mass, liquid, and polymer sensitivity of acoustic wave sensors with viscoelastic guiding layers](#)

*J. Appl. Phys.* **93**, 675 (2003); 10.1063/1.1524309

[Mass sensitivity of acoustic wave devices from group and phase velocity measurements](#)

*J. Appl. Phys.* **92**, 3368 (2002); 10.1063/1.1499750

[Theoretical mass sensitivity of Love wave and layer guided acoustic plate mode sensors](#)

*J. Appl. Phys.* **91**, 9701 (2002); 10.1063/1.1477603

[Surface transverse waves in polymer-coated grating configurations](#)

*J. Appl. Phys.* **91**, 5700 (2002); 10.1063/1.1465502

---



**AIP** | Journal of  
Applied Physics

*Journal of Applied Physics* is pleased to  
announce **André Anders** as its new Editor-in-Chief

## A simple and accurate model for Love wave based sensors: Dispersion equation and mass sensitivity

Jiansheng Liu<sup>a</sup>

*Institute of Acoustics, Chinese Academy of Sciences, Beijing 100190, China*

(Received 4 April 2014; accepted 23 June 2014; published online 1 July 2014)

Dispersion equation is an important tool for analyzing propagation properties of acoustic waves in layered structures. For Love wave (LW) sensors, the dispersion equation with an isotropic-considered substrate is too rough to get accurate solutions; the full dispersion equation with a piezoelectric-considered substrate is too complicated to get simple and practical expressions for optimizing LW-based sensors. In this work, a dispersion equation is introduced for Love waves in a layered structure with an anisotropic-considered substrate and an isotropic guiding layer; an intuitive expression for mass sensitivity is also derived based on the dispersion equation. The new equations are in simple forms similar to the previously reported simplified model with an isotropic substrate. By introducing the Maxwell-Weichert model, these equations are also applicable to the LW device incorporating a viscoelastic guiding layer; the mass velocity sensitivity and the mass propagation loss sensitivity are obtained from the real part and the imaginary part of the complex mass sensitivity, respectively. With Love waves in an elastic SiO<sub>2</sub> layer on an ST-90°X quartz structure, for example, comparisons are carried out between the velocities and normalized sensitivities calculated by using different dispersion equations and corresponding mass sensitivities. Numerical results of the method presented in this work are very close to those of the method with a piezoelectric-considered substrate. Another numerical calculation is carried out for the case of a LW sensor with a viscoelastic guiding layer. If the viscosity of the layer is not too big, the effect on the real part of the velocity and the mass velocity sensitivity is relatively small; the propagation loss and the mass loss sensitivity are proportional to the viscosity of the guiding layer. © 2014 Author(s). All article content, except where otherwise noted, is licensed under a Creative Commons Attribution 3.0 Unported License. [<http://dx.doi.org/10.1063/1.4886773>]

### I. INTRODUCTION

Since Love wave (LW) based sensors were reported in 1992,<sup>1,2</sup> they have been attracting the interest of many researchers. LW is a kind of layered surface acoustic wave (SAW) which is only polarized in the shear horizontal (SH) direction. LW exists in a layered structure with a finite thickness guiding layer deposited on a semi-infinite thickness substrate, and the transverse acoustic wave in the layer is slower than that in the substrate. Due to the guiding layer, the energy of LW is concentrated in the guiding layer and the substrate near the surface; thus LW is very sensitive to the disturbance loaded the surface of the guiding layer and this feature can be used to produce a sensor with good performance. LW-based sensors have the following advantages of high sensitivity, adjustable temperature coefficient, and small coupling loss into liquids, etc. As a kind of SAW sensor, LW-based sensors are significantly different from the commonly used Rayleigh type SAW (RSAW) based sensors. The propagation properties of RSAW mainly depend on the parameters of the piezoelectric substrate, while the properties of LW depend on not only the piezoelectric substrate

---

<sup>a</sup>E-mail address: [liujs98@hotmail.com](mailto:liujs98@hotmail.com)



but also the waveguide layer's characteristics, such as density, velocity of shear acoustic wave, viscoelasticity, and thickness.

Dispersion equation is an important tool for analyzing the propagation properties of acoustic waves in layered structures. Haskell<sup>3</sup> studied the dispersion relation of surface waves on multilayered isotropic medium. Anderson<sup>4</sup> analyzed the dispersion of Love waves in heterogeneous anisotropic materials. Curtis and Redwood<sup>5</sup> gave the conditions for the existence of Love waves in a layered structure with a metal layer on a 6 mm-class piezoelectric material. To achieve the accurate solution of LW, the author<sup>6,7</sup> presented a general dispersion equation which includes the piezoelectricity of the substrate. Using the equation, the calculated dispersive curves and sensitivities agree well with the reported experiment. The shortcoming of the dispersion equation is too complicated to obtain intuitive physically meaningful expressions, which can directly indicate the sensor performance by using the material and structural parameters of LW devices. So some researchers<sup>8-10</sup> would rather use a simple but imprecise theoretical model in which the substrate is treated as an isotropic medium. However, during designing LW-based sensors, the imprecision of the simple model leads to a large deviation in numerical result from the experimental result. To solve the problem, in this work a simple and accurate theoretical model will be presented.

For LW-based sensors, the piezoelectricity of most commonly used substrate such as ST-cut and 90°X-propagate quartz<sup>11-13</sup> is relatively small. But, due to the strong anisotropy of quartz, simplifying the substrate as an isotropic material will result in a great deviation from the exact solution. Based on the above analysis, Zimmermann<sup>14</sup> developed a dispersion equation for LW in a layered structure with an anisotropic-considered substrate and an elastic layer; however, the form of her equation is not suitable to get condensed expressions. In the theoretical part of this study, a detailed inducing process is presented to obtain another form of the dispersion equation for LWs in a layered structure with an anisotropic-considered substrate and an isotropic guiding layer. Compared to the previously reported dispersion equations, the form of the new equation is very close to the dispersion equation with an isotropic-considered substrate. Perturbation theory is applied on the dispersion equation and the mass sensitivity is derived for LW-based sensors. Properties of a LW sensor incorporating a viscoelastic guiding layer are also investigated. The real part and the imaginary part of the complex mass sensitivity correspond to the mass velocity sensitivity and mass loss sensitivity, respectively. In the numerical illustration, the dispersive curves and mass sensitivities of the first two Love modes in the layered structure with an elastic SiO<sub>2</sub> guiding layer on a differently considered quartz substrate are presented. A comparison is carried out between the propagation velocities and mass sensitivities, which prove that the new method can bring accurate solutions close to those of the complicated method with a piezoelectric-considered substrate. Another numerical calculation is carried out for the case of a LW sensor with a viscoelastic guiding layer. If the viscosity of the layer is not too big, the effect on the real part the velocity and the mass velocity sensitivity is relatively small; the propagation loss and the mass loss sensitivity are proportional to the viscosity of the guiding layer.

## II. THEORETICAL MODEL

### A. Dispersion equation for LWs in the layered structure with an anisotropic-considered substrate

As shown in Figure 1, the layered structure considered in this study consists of a semi-infinite thickness substrate and a finite thickness layer. A rectangular Cartesian coordinate system ( $x_1$ ,  $x_2$ , and  $x_3$ ) is chosen in such way that the  $x_1$ -axis is parallel to the direction of LW propagation, the  $x_2$ -axis is in the shear horizontal direction and the  $x_3$ -axis is vertical to the surface of the substrate. The substrate occupies the half-space of  $x_3 \leq 0$ ; the guiding layer occupies the domain of  $0 \leq x_3 \leq h$  and is rigidly linked to the substrate; the space above the layer is occupied by air or vacuum which is assumed no mechanical contact with the guiding layer. In this work, the guiding layer is considered as an isotropic, non-conductive and non-piezoelectric material. The substrate is a piezoelectric material in which the electric field is only coupled with the particle displacement in the  $x_2$  direction. The material matrices of such a material must obey the following

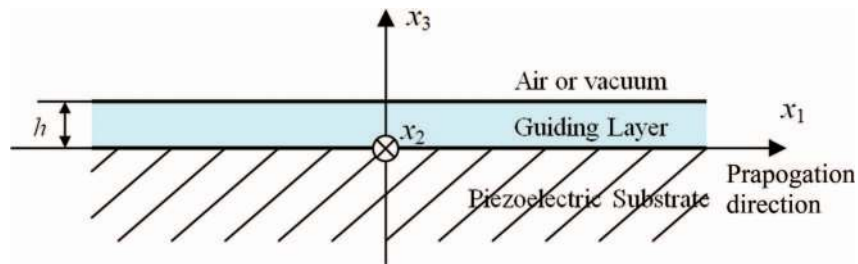


FIG. 1. The schematic of a layered structure supporting Love waves.

structures:<sup>15</sup>

$$\mathbf{c} = \begin{bmatrix} c_{11} & c_{12} & c_{13} & 0 & c_{15} & 0 \\ c_{12} & c_{22} & c_{23} & c_{24} & c_{25} & c_{26} \\ c_{13} & c_{23} & c_{33} & 0 & c_{35} & 0 \\ 0 & c_{24} & 0 & c_{44} & 0 & c_{46} \\ c_{15} & c_{25} & c_{34} & 0 & c_{55} & 0 \\ 0 & c_{26} & 0 & c_{46} & 0 & c_{66} \end{bmatrix} \quad (1)$$

$$\mathbf{e} = \begin{bmatrix} 0 & e_{12} & 0 & e_{14} & 0 & e_{16} \\ e_{12} & e_{22} & e_{23} & e_{24} & e_{25} & e_{26} \\ 0 & e_{23} & 0 & e_{34} & 0 & e_{36} \end{bmatrix}.$$

Here  $\mathbf{c}$  and  $\mathbf{e}$  represent the elastic and piezoelectric constants matrices, respectively.

### 1. Acoustic waves in the substrate and guiding layer

In a homogeneous elastic medium, we consider there is a plane acoustic wave propagating in the  $x_1$  direction and the particle displacement in the  $x_2$  direction. The wave can be expressed as

$$u_2 = A e^{i[\omega t - k(x_1 + i\beta x_3)]}, \quad (2)$$

where  $A$  is the amplitude of the particle displacement,  $\omega$  is the angular frequency,  $k$  is the propagation constant,  $\beta$  is the distribution factor of the particle displacement along the  $x_3$  direction,  $i = \sqrt{-1}$  is an imaginary unit. Obviously, the particle motion must comply with Newton's law:

$$c_{2j2l} \frac{\partial^2 u_2}{\partial x_j \partial x_l} = \rho \frac{\partial^2 u_2}{\partial t^2} \quad (3)$$

where  $\rho$  is the density and  $c_{2j2l}$  is the stiffness coefficient listed in the elastic constants matrix. Substituting Equation (2) into (3), we can get

$$c_{44}\beta^2 - 2ic_{46}\beta - c_{66} + \rho v^2 = 0, \quad (4)$$

where  $v = \omega/k$  is the phase velocity. Equation (4) is a quadratic equation with respect to  $\beta$  and its solutions are:

$$\beta = \frac{ic_{46} \pm \sqrt{c_{44}(c_{66} - \rho v^2) - c_{46}^2}}{c_{44}}. \quad (5)$$

If the expression in the root of Equation (5) is equal to 0, the amplitude of particle displacement along the  $x_3$  direction will remain unchanged, which corresponds to the body acoustic wave propagating in the  $x_1$  direction and particle displacing in the  $x_2$  direction.

In the semi-infinite thick substrate, here which is considered as anisotropic and non-piezoelectric, let the root part in Equation (5) equal to zero, we can get  $V_{S1} = \sqrt{\frac{c_{66} - c_{46}^2/c_{44}}{\rho_s}}$ , which is the velocity

of the quasi-SH acoustic wave in the substrate. To ensure the particle displacement decaying to zero when  $x_3$  tends negative infinity, the real part of  $\beta$  must be positive:

$$\beta_S = \frac{ic_{46}}{c_{44}} + \sqrt{(V_{S1}^2 - v^2)/V_{S2}^2}, \quad (6)$$

where  $V_{S2} = \sqrt{c_{44}/\rho_S}$  is the velocity of the transverse acoustic wave with the propagation in the  $x_3$  direction and the particle displacement in the  $x_2$  direction. In the anisotropic-considered substrate,  $\beta_S$  is a complex number; the real part of  $\beta_S$  denotes the attenuation of the particle displacement along the  $x_3$  direction and the imaginary part indicates angle between the particle motion and the  $x_3$ -axis. Substituting Equation (6) into (2), we can get the solution of SH waves in the substrate:

$$u_{2S} = A_S e^{i[\omega t - k(x_1 + i\beta_S x_3)]} \quad (7)$$

In the finite-thickness guiding layer, which is an isotropic material ( $c_{46} = 0$ ,  $c_{44} = c_{66} = \mu_L$ ), two roots of Equation (4) must be remained:

$$\beta = \pm i\beta_L, \quad (8)$$

where  $\beta_L = \sqrt{v^2/(V_L)^2 - 1}$  and  $k\beta_L$  is the propagation constant of transverse acoustic waves propagating in the  $x_3$  direction.  $V_L = \sqrt{\mu_L/\rho_L}$  is the phase velocity of transverse acoustic waves in the layer. Thus the acoustic wave in the guiding layer can be expressed as:

$$u_{2L} = A_{1L} e^{i[\omega t - k(x_1 - \beta_L x_3)]} + A_{2L} e^{i[\omega t - k(x_1 + \beta_L x_3)]}. \quad (9)$$

$A_S$  in Equation (7) and  $A_{nL}$  in Equation (9) are coefficients to be determined by the boundary conditions.

## 2. Boundary conditions and dispersion equations

There are three undetermined coefficients in Equation (7) and Equation (9), so three boundary equations are needed.

At the plane of  $x_3 = 0$ , the particle displacement in the substrate is equal to that in the layer:

$$A_S = A_{1L} + A_{2L}. \quad (10)$$

At the plane of  $x_3 = 0$ , the stress is continuous in the  $x_3$  direction:

$$(\beta_S c_{44} - ic_{46}) A_S = i\mu_L \beta_L (A_{1L} - A_{2L}). \quad (11)$$

At the plane of  $x_3 = h$ , the stress in the  $x_3$  direction must be zero:

$$i\beta_L (A_{1L} e^{i\beta_L kh} - A_{2L} e^{-i\beta_L kh}) = 0. \quad (12)$$

Substituting Equation (10) into (11), we can get:

$$(\beta_S c_{44} - ic_{46} - i\mu_L \beta_L) A_{1L} + (\beta_S c_{44} - ic_{46} + i\mu_L \beta_L) A_{2L} = 0. \quad (13)$$

Comparing Equation (12) and (13), we can remove the undetermined coefficients and get:

$$-\frac{A_{1L}}{A_{2L}} = \frac{\beta_S c_{44} - ic_{46} + i\beta_L \mu_L}{\beta_S c_{44} - ic_{46} - i\beta_L \mu_L} = -\frac{e^{-i\beta_L kh}}{e^{i\beta_L kh}}. \quad (14)$$

Equation (14) can be further simplified as:

$$\mu_L \beta_L \tan(\beta_L kh) = c_{44} \overline{\beta_S}. \quad (15)$$

where  $\overline{\beta_S} = \sqrt{(V_{S1}^2 - v^2)/V_{S2}^2}$  is the real part of  $\beta_S$ . Equation (15) is the dispersion equation for LWs in a layered structure with an isotropic guiding layer on an anisotropic-considered substrate. In the previous reports,<sup>8,9</sup> the substrate is considered as an isotropic material (assuming  $c_{44} = c_{66}$  and  $c_{46} = 0$ ), thus the dispersion equation is simplified as:

$$\mu_L \beta_L \tan(\beta_L kh) = \mu_S \beta_S, \quad (16)$$

where  $\mu_S$  is the shear modulus of the substrate,  $\beta_S = \sqrt{1 - v^2/V_S^2}$  and  $V_S = \sqrt{\mu_S/\rho_S}$  is the phase velocity of transverse acoustic waves in the substrate which is considered as an isotropic material.

If the substrate is treated as a piezoelectric material, the dispersion equation of LWs becomes:<sup>6</sup>

$$\mu_L \beta_L \tan(\beta_L kh) = \frac{(D_2 - \bar{\epsilon}_L)T_1 - (D_1 - \bar{\epsilon}_L)T_2}{(D_2 - \bar{\epsilon}_L)A_1 - (D_1 - \bar{\epsilon}_L)A_2}. \quad (17)$$

In Equation (17),  $T_1$  and  $T_2$  are the surface normal stresses of the substrate at the plane of  $x_3 = 0$ ;  $D_1$  and  $D_2$  are the substrate surface normal electric displacements at the plane of  $x_3 = 0$ ;  $A_1$  and  $A_2$  are the ratios of the particle displacement amplitude to electric potential amplitude in the substrate,  $\bar{\epsilon}_L$  is the equivalent permittivity of the guiding layer.

In all three equations, the left side represents the transverse acoustic waves propagating in the guiding layer, which is considered as an isotropic material in all three two models, so their left sides have the same form. Equation (15) and (16) have a similar expression of the right side, which represents the acoustic waves propagating in the substrate; however, the physical meaning of each equation is essentially different. In Equation (15),  $V_{S1}$  represents acoustic wave propagating in the  $x_1$  direction;  $c_{44}$  and  $V_{S2}$  represent the acoustic wave propagating along the  $x_3$  direction, namely wave coupled into the guiding layer.  $V_{S1} \neq V_{S2}$  indicates that the substrate is anisotropic. In Equation (16), the substrate is considered as an isotropic material in which transverse acoustic waves propagating along any direction have the same propagation velocity. If the substrate has a strong anisotropy, the isotropy approximation will lead to a large deviation from the exact value. The right side of Equation (17) represents not only the SH acoustic waves in the substrate, but also the electric field in the whole layered structure. Therefore, the right side of Equation (17) is much more complicated than the right side of Equation (15). If the substrate is a material with weak piezoelectricity, the solution of Equation (15) should be very close to the solution of Equation (17).

## B. Mass velocity sensitivity

The dispersion equation (15) can be written in the following form:

$$F(v, h) = \mu_L \beta_L \tan(\beta_L kh) - c_{44} \bar{\beta}_S = 0. \quad (18)$$

In this section, both the substrate and the layer are assumed lossless, thus the propagation number is a real number and  $k = 2\pi/\lambda$ . When a LW device is finished, the wave length  $\lambda$  is fixed by the period of the interdigital transducer (IDT); thus the propagation factor  $k$  is a constant in Equation (18). Assuming there is a small increase of  $\Delta h$  in the guiding layer thickness, which will result in a change of  $\Delta v$  in the propagation velocity:

$$F(v + \Delta v, h + \Delta h) = 0. \quad (19)$$

Expanding Equation (19) into the Taylor series about the point  $(v, h)$  with respect to a small increment of  $(\Delta v, \Delta h)$  and, neglecting terms higher than the first order, we can get:

$$F(v + \Delta v, h + \Delta h) = F(v, h) + \left. \frac{\partial F}{\partial v} \right|_{(v,h)} \cdot \Delta v + \left. \frac{\partial F}{\partial h} \right|_{(v,h)} \cdot \Delta h = 0 \quad (20)$$

From Equation (20), we can obtain:

$$\Delta v = - \left. \frac{\partial F / \partial h}{\partial F / \partial v} \right|_{(v,h)} \cdot \Delta h. \quad (21)$$

Substituting Equation (18) into (21), we can get:

$$\Delta v = - \frac{\mu_L \beta_L^2 / \rho_L v h}{1 + \frac{1}{\beta_L kh} \sin(\beta_L kh) \cos(\beta_L kh) + \frac{\rho_S / \rho_L}{\beta_S kh} \cos^2(\beta_L kh)} \cdot \Delta h \quad (22)$$

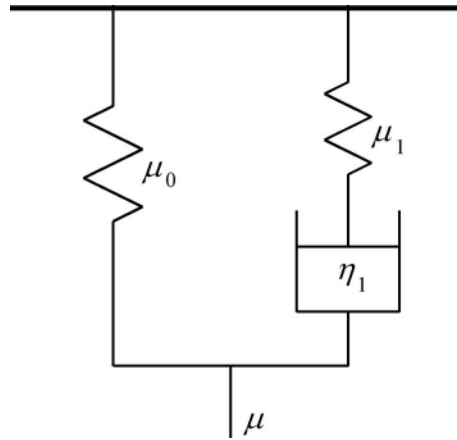


FIG. 2. Schematic of the Maxwell-Weichert model for the viscoelastic guiding layer.

When a mass load is acted on the surface of the guiding layer, similar to the reported change<sup>6</sup> in dispersion Equation (17), dispersion Equation (15) becomes:

$$\mu_L \beta_L \frac{\mu_L \beta_L \tan(\beta_L kh) + k\sigma v^2}{\mu_L \beta_L - k\sigma v^2 \tan(\beta_L kh)} = c_{44} \overline{\beta_S}, \quad (23)$$

where  $\sigma$  is the areal density of the mass load. If  $\sigma$  tends to zero,  $k\sigma v^2 / \mu_L \beta_L = \tan(k\sigma v^2 / \mu_L \beta_L)$  and Equation (23) becomes:

$$\mu_L \beta_L \tan \left[ \beta_L k \left( h + \frac{\sigma v^2}{\mu_L \beta_L^2} \right) \right] = c_{44} \overline{\beta_S}. \quad (24)$$

Equation (24) indicates that a tiny mass  $\sigma$  loaded on the guiding layer surface can be equivalent to an increment in the guiding layer thickness and

$$\Delta h = \frac{\sigma v^2}{\mu_L \beta_L^2}. \quad (25)$$

Substituting Equation (25) into (22), we can get the mass velocity sensitivity of LW-based sensors:

$$S_m^v = \left. \frac{\Delta v}{v\sigma} \right|_{\sigma \rightarrow 0} = -\frac{1}{\rho_L h} \cdot \frac{1}{1 + \frac{1}{\beta_L kh} \sin(\beta_L kh) \cos(\beta_L kh) + \frac{\rho_S/\rho_L}{\beta_S kh} \cos^2(\beta_L kh)}. \quad (26)$$

Equation (26) has a similar form to the previous reported mass sensitivity<sup>16</sup> for LW-based sensors with an isotropic-considered substrate.

### C. LW sensors incorporating viscoelastic layers

If the guiding layer is an elastic material, the velocity and the mass sensitivity of a LW sensor can be obtained by using the equations presented in the previous section. To achieve a higher mass sensitivity, polymers are often adopted as guiding materials of LW devices because of their lower velocity of transverse waves and less density. Different from elastic overlays, a polymer guiding layer will produce a large propagation attenuation because of its non-ignorable viscosity. When the viscoelasticity is considered, the shear modulus  $\mu_L$  of the guiding layer becomes a complex variant. The mechanical behavior of a viscoelastic material can be described by using a model consisting of springs and dashpots. In this work, a simplified Maxwell-Weichert model (seen in Figure 2) is

TABLE I. Material parameters of simplified model used in numerical calculation.

Parameters	ST-90°X quartz	SiO <sub>2</sub>
$\rho$ in kg/m <sup>3</sup>	2651	2200
$c_{44}$ in GPa	30.34	
$c_{66}$ in Gpa	67.47	
$c_{46}$ in Gpa	-7.60	
$c_{66} - c_{46}^2/c_{44}$ in Gpa	65.57	
$V_{S1}$ in m/s	4973	
$V_{S2}$ in m/s	3383	
$V_{SSBW}$ in m/s	4992	
$\mu_L$ in Gpa		17.40
$V_L$ in m/s		2812

adopted; thus the complex shear modulus can be expressed as:<sup>17</sup>

$$\mu_L = \mu_0 + \mu_1 \frac{i\omega\tau_1}{1 + i\omega\tau_1} \quad (27)$$

where  $\tau_1 = \eta_1/\mu_1$  is the relaxation time of the Maxwell branch. Substituting the complex  $\mu_L$  into the dispersion equations, we can get a complex velocity  $v = v_r + iv_i$ .  $v_r$  represents the propagation velocity in the  $x_1$  direction,  $v_i$  is related to the propagation loss in the  $x_1$  direction:

$$IL \approx -40\pi (\log_{10} e) \frac{v_i}{v_r} = -54.6 \frac{v_i}{v_r}, \quad (28)$$

The mass sensitivity calculated by using Equation (26) is also a complex number:

$$S_m^v = \frac{\Delta v}{v\sigma} \Big|_{\sigma \rightarrow 0} \approx \frac{\Delta v_r + i\Delta v_i}{v_r\sigma} \Big|_{\sigma \rightarrow 0} = S_m^{v_r} - i \frac{S_m^{IL}}{54.6}, \quad (29)$$

where  $S_m^{v_r}$  mass velocity sensitivity of a LW sensor incorporating a viscoelastic guiding layer,  $S_m^{IL}$  is the mass insertion loss sensitivity.

### III. ILLUSTRATIONS OF LWS IN A DEVICE WITH A QUARTZ SUBSTRATE

#### A. LWS in a structure with an elastic layer

To verify the accuracy of the new dispersion equation and sensitivity, numerical calculations are carried out by using the equations listed in the previous section. The analyzed LW-based sensor consists of a substrate of ST-90°X quartz and an elastic guiding layer of silicon oxide. It is known that ST-cut quartz is a piezoelectric material, which supports a Rayleigh wave parallel to the X-axis and a surface skimming bulk wave (SSBW) perpendicular to the X-axis.<sup>18</sup> The material constants of quartz are from reference.<sup>19</sup> It is noted that the given material constants are based on crystal axis coordinates, which is different from the calculation coordinates shown in Figure 1. To obtain the material constants in the calculation coordinates, a Bond transformation is needed and the Euler angles of ST-90°X quartz are (0, 132.75°, 90°). Due to the very low propagation loss and good abrasion resistance, SiO<sub>2</sub> is considered as an ideal material for the guiding layer of LW-based devices. In LW mode sensors, SiO<sub>2</sub> is usually sputtered on the substrate surface and its material constants<sup>2</sup> are slightly different from the constants of fused quartz. The density and the elastic constants of the substrate and the guiding layer are listed in Table I. As shown in Table I,  $c_{44}$  is much different from  $c_{66}$ , which indicates ST-90°X quartz has a strong anisotropy. The strong anisotropy will lead to a big deviation in the solution of isotropic-considered substrate to the exact solution, which will be verified in the following numerical results.

In Figure 3(a) and 4(a), the black curves represent the propagation velocity and mass velocity sensitivity of LWS in a device incorporating a piezoelectric-considered quartz substrate; the blue curves represent the velocity and the sensitivity with an anisotropic-considered substrate; the red



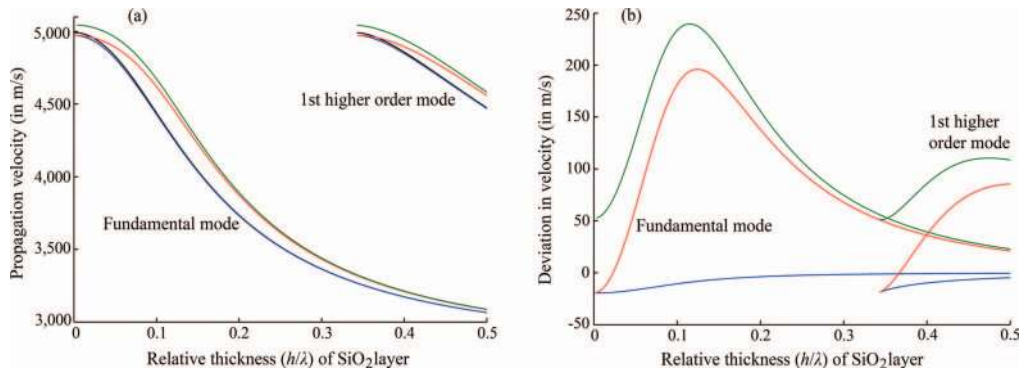


FIG. 3. Comparison between the propagation velocities of the first two Love modes in a device with an elastic SiO<sub>2</sub> layer on a differently considered ST-90°X quartz substrate. (a) Propagation velocity vs. relative guiding layer thickness, (b) Deviations of propagation velocity with differently simplified substrate from the exact values.

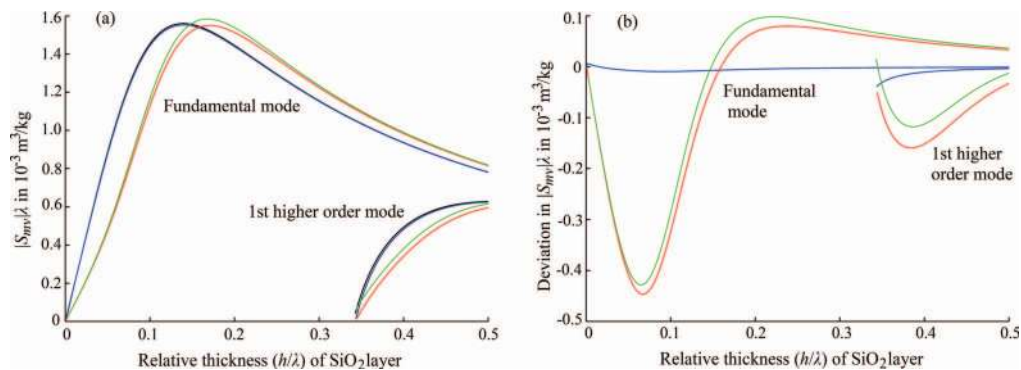


FIG. 4. Comparison between the magnitudes of normalized mass velocity sensitivity for the first two Love modes in a device with an elastic SiO<sub>2</sub> layer on a differently considered ST-90°X quartz substrate. (a) The magnitudes of normalized sensitivity vs. relative guiding layer thickness, (b) Deviations of the sensitivity with differently simplified substrate from the exact values.

curves represent the velocity and the sensitivity with an isotropic-considered substrate and  $\mu_S = c_{66} - c_{46}^2/c_{44}$ ; the green curves represent the velocity and the sensitivity with an isotropic-considered substrate and  $\mu_S = c_{66}$ . In Figure 3(b) and 4(b), the blue, red, green curves represent the velocity and sensitivity deviations of differently simplified substrate to the exact solutions with a piezoelectric-considered substrate.

In Figure 3, the propagation velocities of LWs in SiO<sub>2</sub>/quartz structure are compared between different-considered substrates. When the guiding layer is very thin, the black curve tends to  $V_{SSBW}$ , the blue and the red curves tend to  $V_{S1}$ , the green curve tends to  $V_S = \sqrt{c_{66}/\rho_S}$ . If thickening the guiding layer, all the propagation velocities decrease and tend to  $V_L$  as the guiding layer tends infinite thick. Figure 3(a) displays that the blue curves are very close to the black curves, which represent the exact theoretical velocities with a piezoelectric-considered substrate. This proves that the method developed in this work has a good accuracy. To clearly compare the accuracy of the dispersion equations with differently simplified substrate, Figure 3(b) shows the deviations in propagation velocities of the first two Love modes from the exact propagation velocities (black curves in Figure 3(a)). The deviation denoted by the blue curves is the smallest and the deviation is being reduced when the guiding layer thickness increases. The deviations denoted by the red curves and the green curves are much bigger, and initially the deviations is increased when the guiding layer thickness increases. The green curves illustrate that the maximum deviation in the velocity of the fundamental Love mode is about 250 m/s (200 m/s for the red curves), which is about 5% (4%) of the propagation velocity. More unfortunately, the maximum deviation occurs at the relative guiding

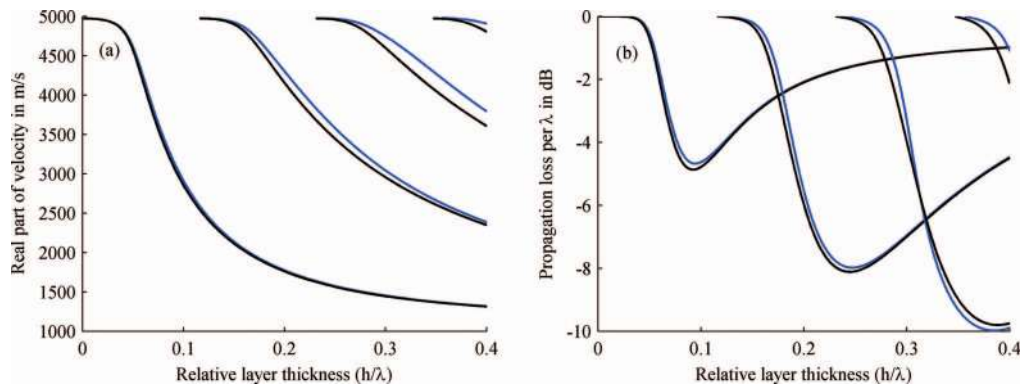


FIG. 5. The real part of velocity and propagation loss vs. relative layer thickness for a LW device with a viscoelastic guiding layer. (a) real part of velocity; (b) propagation loss. The black lines in (b) denote the propagation loss scaled up by a factor of 1000.

layer thickness of 12%, which is the most valuable for LW-based sensors because of closing to the layer thickness corresponding to the maximum sensitivity (seen in Figure 4(a)).

In Figure 4, the normalized mass velocity sensitivities of the first two Love modes with different-considered substrate are compared. The blue curves in Figure 4(a) almost completely overlap with the black curves, which illustrates that we can get a very precise sensitivity of LW-based sensors by using Equation (26) with an anisotropic-considered substrate. The red and the green curves are deviated from the black curves obviously, although their maximum values are very close. The maximum sensitivity represented by the blue and the black curves occurs at the relative guiding layer thickness of 14%, while the maximum sensitivity represented by the red and the green curves occurs at the relative guiding layer thickness of 17%. Before reaching the maximum value, the blue and the black curves have been above the red and the green curves. Figure 4(b) shows the deviations in the normalized mass velocity sensitivity of differently simplified method to the exact values. The blue curve shows that the sensitivity calculated by using the model with an anisotropic-considered substrate has an excellent accuracy. The red curves and the green curves illustrate that the model with an isotropic-considered substrate has a worse accuracy. For the red curves, the maximum deviation in the normalized sensitivity of the fundamental Love mode is about  $0.45 \times 10^{-3} \text{ m}^3/\text{kg}$  ( $0.43 \times 10^{-3} \text{ m}^3/\text{kg}$  for the green curves), which is about the 28% of the maximum normalized sensitivity.

## B. LWs in a structure with a viscoelastic guiding layer

In the followings some numerical results will be presented for a LW device incorporating a viscoelastic guiding layer on an anisotropic-considered ST-90°X quartz substrate. The device is characterized by a wavelength of  $40 \mu\text{m}$ , which is decided by the period of the interdigital transducers deposited on the substrate surface. Material parameters of the viscoelastic layer are assumed as:  $\rho_L = 1200 \text{ kg/m}^3$ ,  $\mu_0 = 1.5 \text{ GPa}$ ,  $\tau_1 = 13 \text{ ns}$ . In Figure 5 and 6, the blue lines correspond to  $\mu_1 = 0.15 \text{ GPa}$ , black lines corresponds to  $\mu_1 = 0.15 \text{ MPa}$ .

As shown in Figure 5(a), the effect on real part of velocity ( $v_r$ ) is relatively small. The blue lines is above the black lines because the shear modulus of the guiding layer with  $\mu_1 = 0.15 \text{ GPa}$  is larger than that with  $\mu_1 = 0.15 \text{ MPa}$ . The impact on the fundamental mode is smaller than on the higher order modes. The difference of the initial layer thicknesses of two adjacent modes is about  $\frac{\lambda/2}{\sqrt{v_{s1}^2/v_L^2 - 1}}$ . Figure 5(b) displays that the effect of layer viscosity on the propagation loss is considerably larger than on the real part of velocity. The black curves are very close to the blue curves, which represent the propagation loss multiplied a factor of 1000, the ratio of corresponding  $\mu_1$ . This result proves that the propagation loss is proportional to the guiding layer viscosity for LW devices incorporating a polymer overlay with a not too big viscosity. Figure 5(b) also shows that the propagation loss of a higher order mode is larger than that of a lower order mode.

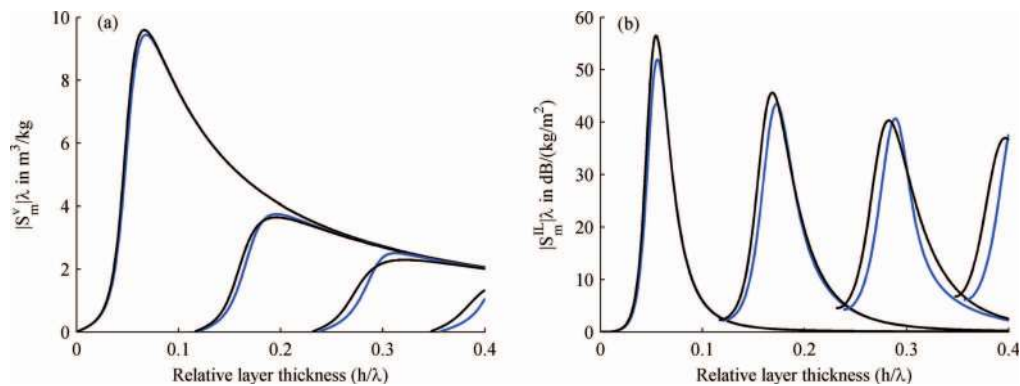


FIG. 6. Magnitudes of normalized  $S_m^V$  and  $S_m^L$  vs. relative layer thickness for a LW device with a viscoelastic guiding layer. The blue lines in (b) represent the mass loss sensitivity multiplied by a factor of 1000.

Figure 6 displays the magnitudes of the normalized mass velocity sensitivity and normalized mass loss sensitivity as functions of the normalized layer thickness. Similar to on the propagation velocity, the effect on the velocity sensitivity is very small and the effect on the fundamental mode is smaller than on the higher modes (seen in Figure 6(a)). The mass sensitivity of a lower order mode is larger than that of a higher order mode. The blue curves in Figure 6(b) represent the normalized mass loss sensitivity multiplied by the factor of 1000. The black curves are very close to the blue curves. This proves that the mass loss sensitivity is also proportional to the viscosity of the guiding layer. The maximum mass loss sensitivity of a lower order mode is larger than that of a higher order mode.

#### IV. CONCLUSIONS

To achieve simple and precise solution, a dispersion equation is induced for LWs in a layered structure with an anisotropic-considered substrate and an isotropic guiding layer; a direct expression of mass velocity sensitivity is also presented based upon the dispersion equation. The simple forms of the dispersion equation and sensitivity expression are similar to those of LWs in the layered structure with an isotropic-considered substrate. With an example of LWs in a commonly used structure with a substrate of ST-90°X quartz and a guiding layer of  $\text{SiO}_2$ , propagation velocities and normalized mass sensitivities are calculated and compared by using different theoretical models. Numerical results show that the method presented in this work can achieve much more accurate solutions than the simplified model reported previously. Another numerical illustration is presented for a LW sensor incorporating a viscoelastic guiding layer on an anisotropic-considered quartz substrate. The calculation results show that the guiding layer viscosity causes a relatively small effect on the real part of velocity and the mass velocity sensitivity; the propagation loss and the mass loss sensitivity are proportional to the viscosity of the guiding layer.

#### ACKNOWLEDGMENTS

The author would like to thank Chinese National Natural Science Foundation for financial support (No. 11104314).

- <sup>1</sup>E. Gizeli, A. C. Stevenson, N. J. Goddard, and C. R. Lowe, *IEEE Trans. Ultrason. Ferroelectr. Freq. Control* **39**, 657 (1992).
- <sup>2</sup>G. Kovacs, G. W. Lubking, M. J. Vellekoop, and A. Venema, in *IEEE 1992 Ultrason. Symp.*, Proceedings. Tucson, 1992, edited by B. R. McAvoy (IEEE, Piscataway, NJ, 1992), p. 281.
- <sup>3</sup>N. A. Haskell, *Bull. Seism. Soc. Am.* **43**, 17 (1953).
- <sup>4</sup>D. L. Anderson, *Geophysics* **27**, 445 (1962).
- <sup>5</sup>R. G. Curtis and M. Redwood, *J. Appl. Phys.* **44**, 2002 (1973).
- <sup>6</sup>J. Liu and S. He, *Int. J. Solids Struct.* **47**, 169 (2010).
- <sup>7</sup>J. Liu and S. He, *J. Appl. Phys.* **107**, 073511 (2010).

- <sup>8</sup>Z. Wang, J. D. N. Cheeke, and C. K. Jen, *IEEE Trans. Ultrason. Ferroelectr. Freq. Control* **43**, 844 (1996).
- <sup>9</sup>G. McHale, M. I. Newton, and F. Martin, *J. Appl. Phys.* **91**, 9701 (2002).
- <sup>10</sup>G. Machale, Michael Ian Newton, and Fabrice Martin, *J. Appl. Phys.* **93**, 675 (2003).
- <sup>11</sup>M. I. Newton, P. Roach, and G. McHale, *Sensors* **8**, 4384 (2008).
- <sup>12</sup>V. Raimbault, D. Rebière, C. Déjous, M. Guirardel, and V. Conedera, *Sens. Actuators A* **142**, 160 (2008).
- <sup>13</sup>L. Fadel, C. Zimmermann, I. Dufour, C. Déjous, D. Rebière, and J. Pistré, *IEEE Trans. Ultrason. Ferroelectr. Freq. Control* **52**, 297 (2005).
- <sup>14</sup>C. Zimmermann, D. Rebière, C. Déjous, J. Pistré, E. Chastaing, and R. Planade, *Sens. Actuators B* **76**, 86 (2001).
- <sup>15</sup>B. Jakoby and M. J. Vellekoop, *Smart Mater. Struct.* **6**, 668 (1997).
- <sup>16</sup>Z. Wang, J. D. N. Cheeke, and C. K. Jen, *Appl. Phys. Lett.* **64**, 2940 (1994).
- <sup>17</sup>J. Liu, L. Wang, Y. Lu, and S. He, *Smart Mater. Struct.* **22**, 125034 (2013).
- <sup>18</sup>C. K. Campbell, *Surface Acoustic Wave Devices for Mobile and Wireless Communications*, (Academic Press, New York, 1998).
- <sup>19</sup>B. A. Auld, *Acoustic fields and waves in solids* (John Wiley, New York, 1973), Vol. 1.